

The DWARF project



P.-E. Christopoulou
Ass. Prof, Dept. of Physics,
University of Patras



ΠΑΝΕΠΙΣΤΗΜΙΟ
ΠΑΤΡΩΝ
UNIVERSITY OF PATRAS

11th HELLENIC ASTRONOMICAL CONFERENCE
Athens, 8 - 12 September 2013



PROJECT DWARF

Initiated and organized by **Dr. Th. Pribulla**, Astronomical Institute
Slovak Academy of Sciences

The DWARF project:

Eclipsing binaries - precise clocks to discover exoplanets

T. Pribulla^{1,*}, M. Vaňko¹, M. Ammler - von Eiff², M. Andreev^{3,4}, A. Aslantürk⁵, N. Awadalla⁶,
D. Baluďanský⁷, A. Bonanno⁸, H. Božić⁹, G. Catanzaro⁸, L. Çelik^{10,11}, **P.E. Christopoulou**¹²,
E. Covino¹³, F. Cusano¹⁴, D. Dimitrov¹⁵, P. Dubovský¹⁶, E.M. Esmer^{10,11}, A. Frasca⁸, Ľ. Hambálek¹,
M. Hanna⁶, A. Hanslmeier¹⁷, B. Kalomeni¹⁸, D. P. Kjurkchieva¹⁹, V. Krushevskaja²⁰, I. Kudzej¹⁶,
E. Kundra¹, Yu. Kuznyetsova²⁰, J.W. Lee²¹, M. Leitzinger¹⁷, G. Maciejewski²², D. Moldovan²³,
M.H.M. Morais²⁴, M. Mugrauer²⁵, R. Neuhauser²⁵, A. Niedzielski²², P. Odert¹⁷, J. Ohlert^{26,27},
İ. Özavcı^{10,11}, **A. Papageorgiou**¹², Š. Parimucha²⁸, S. Poddany^{29,30}, A. Pop²³, M. Raetz³¹, S. Raetz²⁵,
Ya. Romanyuk⁴, D. Ruždjak⁹, J. Schulz³², H.V. Şenavcı^{10,11}, T. Szalai³³, P. Székely³⁴, D. Sudar⁹,
C.T. Tezcan^{10,11}, M.E. Törün^{10,11}, V. Turcu²³, O. Vince³⁵, and M. Zejda³⁵

22-7-2013 727 planetary systems / 942 planets / 146 multiple planet systems

- S-Type the planet moves around one of the two stars
- P-Type the planet moves around the entire binary- **circum-binary planets**
(Mutterspough et al. 2007)

Simulations show either of above possibilities has a large range of stable configurations
(see e.g., Broucke 2001; Pilat-Lohinger & Dvorak 2002; Pilat-Lohinger et al. 2003; Benest
2003 Moriwaki & Nakagawa 2004; Quintana & Lissauer 2006; Pierens & Nelson 2008).

HOW we detect
circubinary planets?

FAR FROM EASY

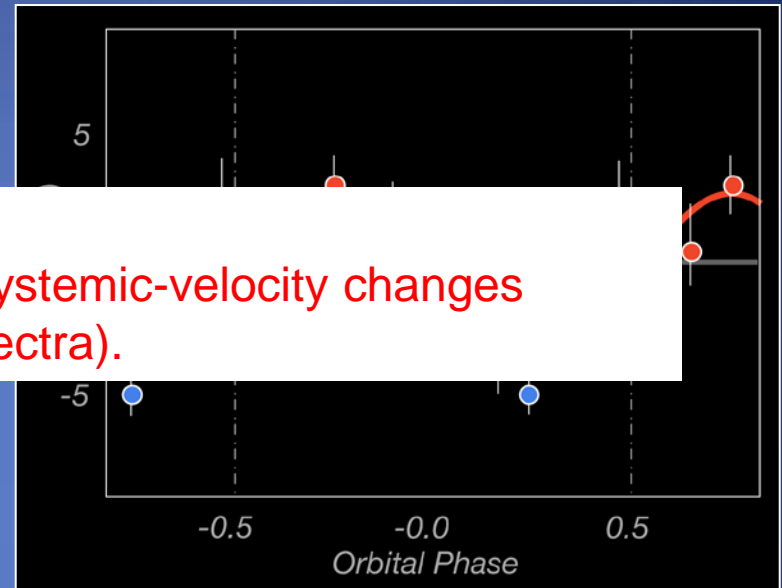
Three principal Techniques

1. Precise radial velocity measurements to detect the wobble of the binary mass center (Konacki et al. 2009)



RV precision insufficient...

There are hardly any binaries where the systemic-velocity changes revealed a third component (unseen in spectra).



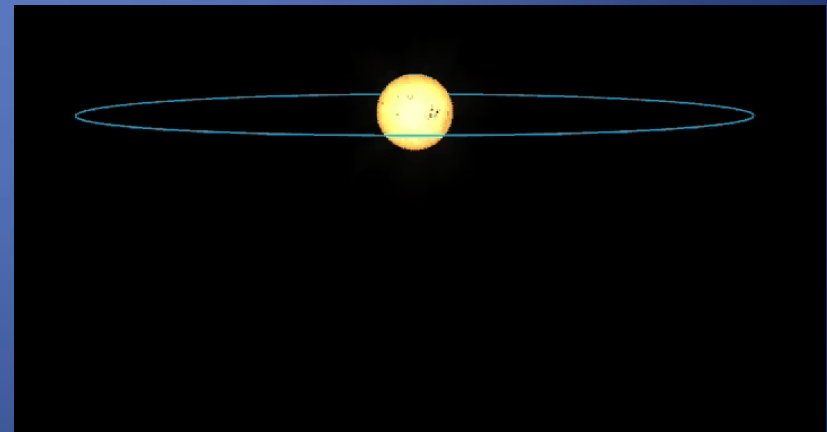
2. Photometric detection of transits of the planets (s) across the disk of the components of the inner binary (Doyle et al. 2011)

Very long photometric runs with excellent accuracy

3 systems

Kepler-16b (Doyle et al., 2011),

Kepler-34b and Kepler-35b (Welsh et al. 2012).



3. Timing of the inner binary eclipses (Lee et al. 2009)

2. Previous and ongoing searches of circumbinary exoplanets by timing technique



Pulse arrival time (PSR1257+12, Wolszczan & Frail, 1992).

Timing of the eclipses in binary stars LITE

- (*Pribulla & Rucinski, 2006; Beuermann et al. 2011*)




Existence of low mass planetary binaries

- CM Dra (*Deeg et al. 2008; Ofir 2008*)
- HW Vir (a short-period EB system composed of an sdB and an M dwarf with two-planets (*Lee et al. 2009, Horner et al. 2012*))

Around post common envelope systems (WD+MS latetype

By March 23 2012 11 planetary systems (16 planets/4 multiple systems) detected by timing

- 
- NN SE (*Beuermann et al. 2010*), UZ For (*Potter et al. 2011*), DP Leo (*Qian et al. 2010*), RR Cae (*Qian et al. 2012*).



The only larger initiative....SOLARIS global network of four 50cm robotic telescopes (Australia, Africa and South America) (*Konacki et al. 2011*).

The Archival DATA play important role (...long periods)

Krakow database prepared and frequently updated by Prof. Kreiner
(<http://www.as.up.krakow.pl/ephem/>)



The screenshot shows the website of the Mt. Suhora Astronomical Observatory, Cracow Pedagogical University. The header includes the observatory's name and a logo. Below the header is a navigation bar with links: (O-C) Atlas, Linear ephemerides, Statistics of minima database, Add new minima, and W UMa stars. A sub-navigation bar contains links: All stars in one file (TXT), allstars.cat (ASCII), SIMBAD, GCVS, and Old ephemerides. The main content area is titled 'UP-TO-DATE LINEAR ELEMENTS OF ECLIPSING BINARIES' and is prepared by J.M. Kreiner. It lists a comprehensive set of star abbreviations (And, Ant, Aps, Aqr, Aql, Ara, Ari, Aur, Boo, Cae, Cam, Cnc, CVn, Cma, Cmi, Cap, Car, Cas, Cen, Cep, Cet, Cha, Cir, Com, Col, CrA, CrB, Crv, Crt, Cru, Cyg, Del, Dor, Dra, Equ, Eri, For, Gem, Gru, Her, Hor, Hya, Hyi, Ind, Lac, Leo, LMi, Lep, Lib, Lup, Lyn, Lyr, Men, Mic, Mon, Mus, Nor, Oct, Oph, Ori, Pav, Peg, Per, Phe, Pic, Psc, PsA, Pup, Pyx, Ret, Sge, Sgr, Sco, Scl, Sct, Ser, Sex, Tau, Tel, Tri, TrA, Tuc, UMa, UMi, Vel, Vir, Vol, Vul). Below the list are links for 'Stars near eclipse', 'Eccentric orbit stars', and 'Other stars'. A paragraph describes the database's origin and includes a citation request. A red text box at the bottom states: 'Current orbital phase is calculated based on YOUR COMPUTER TIME !!!!'.

UP-TO-DATE LINEAR ELEMENTS OF ECLIPSING BINARIES

prepared by J.M. Kreiner, sfkreine@cyf-kr.edu.pl

And | Ant | Aps | Aqr | Aql | Ara | Ari | Aur | Boo | Cae | Cam | Cnc | CVn | Cma | Cmi | Cap | Car | Cas | Cen | Cep | Cet | Cha | Cir | Com | Col | CrA | CrB | Crv | Crt | Cru | Cyg | Del | Dor | Dra | Equ | Eri | For | Gem | Gru | Her | Hor | Hya | Hyi | Ind | Lac | Leo | LMi | Lep | Lib | Lup | Lyn | Lyr | Men | Mic | Mon | Mus | Nor | Oct | Oph | Ori | Pav | Peg | Per | Phe | Pic | Psc | PsA | Pup | Pyx | Ret | Sge | Sgr | Sco | Scl | Sct | Ser | Sex | Tau | Tel | Tri | TrA | Tuc | UMa | UMi | Vel | Vir | Vol | Vul

[Stars near eclipse](#) | [Eccentric orbit stars](#) | [Other stars](#)

The database is described in the paper: "Up-to-date Linear Elements of Close Binaries", J.M. Kreiner, 2004, Acta Astronomica, vol. 54, pp 207-210. **Please include a citation when using the database for your research.** This project was partly supported by KBN grant No 2 P03D 006 22.

Current orbital phase is calculated based on YOUR COMPUTER TIME !!!!

Advantages

- it is complementary to the competing project SOLARIS covering the Southern hemisphere
- it uses only existing facilities
- unlike other projects it would cover relatively extensive list of targets increasing chance of new detection(s)
- it is a unique collaboration of many observatories

3. Target Selection

objects with sharp and deep minima

- (i) systems with K or/and M dwarf components
- (ii) systems with hot subdwarf (sdB or sdO) and K or M dwarf components
- iii) post-common envelope systems with a white dwarf (WD) component

NSVS data (Hoffman et al., 2008),
HAT network data (Hartman et al., 2011) and
ASAS data (see Pojmanski, 2002; Pojmanski 2003, Pojmanski &
Maciejewski, 2004ab; Pojmanski et al., 2005)

Objects North of DEC = -10° with $P < 5$ d , $R = 10-17$ mag

Maximum amount of information but also neglected systems.
Follow up observations...

Preliminary target list

Table 1 Target list

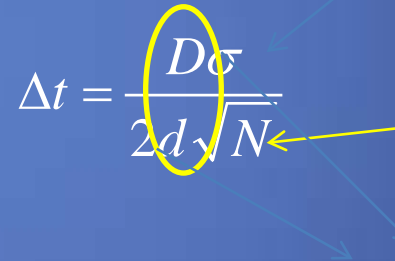
Target	α_{2000}	δ_{2000}	M_1 [M_\odot]	M_2 [M_\odot]	Sp.type	A_{OCC} [mag]	ΔT [s]	HJD _I 2 400 000+	Period [days]	d_I [mag]	d_{II} [mag]	D_I [days]	<i>V</i>	<i>R</i>	Δt [s]	N_σ	Ref
DV Psc	00 13 09.2	+03 35 43	0.49	0.51	K3V+M1V	0.04	4.5	52500.1150	0.30833740	0.32	0.15	0.062	10.6	10.0	1.1	4.1	(1)
PTFEB11.441	00 45 46.0	+41 50 30	0.51	0.35	M3.5+WD		5.0	55438.3165	0.35871000	0.20	0.00			16.3			(2)
NSVS 06507557	01 58 23.9	+25 21 20	0.66	0.28	K9+M3		4.7	54746.3801	0.51508836	0.70	0.23	0.062	13.4	12.6	1.8	2.6	(3)
BX Tri	02 20 50.8	+33 20 48	0.51	0.26	M1V+M4V	0.03	5.4	51352.0616	0.19263590	0.33	0.27	0.072	13.4	12.5	4.2	1.3	(4)
V449 Per	02 57 33.5	+35 14 01						52500.9069	0.94620690					12.5			(5)
GJ 3236	03 37 14.1	+69 10 50	0.38	0.28	M4V	0.02	5.9	54734.9959	0.77126000	0.21	0.19	0.039	14.0	13.5	6.3	0.9	(6)
V912 Per	03 44 32.2	+39 59 35						53287.8523	0.57759120	0.22	0.20			13.1			(9)
NLTT11748	03 45 16.8	+17 48 09	0.28	0.27	WD+WD		6.6	55619.4264	0.11601549	0.55	0.11		16.7	16.3			(7)
V471 Tau	03 50 25.0	+17 14 47			K2V+DA			52500.3434	0.52118357	0.03	0.00		9.5	9.5			(8)
HAT-216-0003316	04 40 23.0	+31 26 46			M4V+M5V			54471.3745	2.04813610				15.2	13.3			(9)
AP Tau	04 54 45.0	+26 55 24						52500.1267	0.97197470				13.0				(5)
HAT-131-0026711	05 16 36.9	+48 35 44						54497.1710	0.66395310	0.30	0.10		14.3				(9)
HAT-133-0002525	06 36 25.2	+43 49 47				0.03		53632.4735	1.59457150	0.40	0.16	0.096	13.8		4.8		(9)
V470 Cam	07 10 42.1	+66 55 44	0.48	0.13	sdB+M	0.04	6.3	51822.7598	0.09564665	1.00	0.20	0.015	14.7	14.6	1.2	5.4	(10)
YY Gem	07 34 37.4	+31 52 10	0.60	0.60	dM1e	0.06	4.0	52500.4573	0.81428330	0.55	0.50		10.6	9.1			(11)
HAT-136-0003262	08 11 34.8	+43 02 33						53770.8395	0.64948470	0.60	0.65	0.071	14.3		3.4		(9)
GSC 1941 1746	08 25 51.9	+24 27 04	0.56	0.65	M2V+M2V		4.0	53730.7303	2.26560000	0.90	0.40	0.453	12.9		3.0	1.3	(12)
CU Cnc	08 31 37.6	+19 23 39	0.43	0.40	M5Vb	0.03	5.1	50208.5068	2.77146800	0.13	0.11	0.083	12.1	11.4	6.1	0.8	(13)
NSVS 02502726	08 44 11.0	+54 23 47	0.71	0.35	K5V+M1V	0.04	4.3	54497.5502	0.55975500	0.50	0.35	0.084	14.0	13.4	3.9	1.1	(14)
GSC 2499 246	09 16 12.3	+36 15 34	0.68	0.73	M3V+M3V		3.6	53456.6763	0.36697100	0.90	0.60	0.070	12.5		1.0	3.6	
HAT-225-0003429	09 21 28.4	+33 25 59				0.02		54534.1898	0.42647590	0.28	0.27	0.047	14.5		6.6		(9)
BS UMa	11 25 41.0	+42 34 50			K9-M1V	0.10		52500.3477	0.34950990	0.41	0.35	0.059	12.5	11.5	2.0		(16)
HW Vir	12 44 20.2	-08 40 17	0.48	0.14	sdB+M6-7		6.2	52500.0560	0.11671947	0.80	0.15	0.014	10.5		0.2	31.0	(17)
DE CVn	13 26 53.3	+45 32 47	0.51	0.41	M3V+DA		4.8	52784.5533	0.36413940	0.10	0.00		12.8	12.2			(18)
NY Vir	13 38 48.1	-02 01 49	0.50	0.15	sdB+M5		6.0	52500.0594	0.10101598	0.90	0.15	0.012	13.3	13.5	0.6	10.0	(10)
NSVS 01031772	13 45 34.9	+79 23 48	0.54	0.50	M2V	0.02	4.4	53456.6796	0.36814140	0.60	0.60	0.055	12.6	11.0	0.8	5.2	(19)
HAT-145-0001586	13 45 13.2	+46 18 40				0.01		53843.9266	1.58752710	0.65	0.55	0.064	14.3		3.1		(9)
GK Boo	14 38 20.7	+36 32 25			K2V	0.04		52500.4350	0.47777170	0.92	0.77	0.091	10.6	10.5	0.5		(20)
GU Boo	15 21 54.8	+33 56 09	0.60	0.59	M0/M1.5	0.15	4.0	52723.9811	0.48871000	0.90	0.65	0.064	13.1	12.9	1.2	3.2	(21)
NSVS 07826147	15 33 49.4	+37 59 28	0.38	0.11	sdB+M5		7.2	54524.0195	0.16177042	1.35	0.20	0.016	13.0	13.4	0.4	18.1	(15)
G179-55	15 47 27.4	+45 07 51	0.26	0.26	M4		7.0	51232.8953	3.55001840	0.05	0.06		12.5				(9)
NN Ser	15 52 56.1	+12 54 45	0.54	0.11	DAO1+M4		6.0	52500.1209	0.13008015	>2	0.00		16.7				(22)
HAT-192-0001841	16 12 16.7	+41 13 51				0.02		53853.9056	0.30873570	0.62	0.55	0.037	14.0		2.1		(9)
CM Dra	16 34 20.4	+57 09 44	0.23	0.21	M4.5V	0.03	7.7	52500.7177	1.26839010	0.75	0.60	0.038	12.9	10.9	9.9	0.8	(23)
TrES-Her0-07621	16 50 20.7	+46 39 01	0.49	0.49	M3V+M3V		4.6	53139.7495	1.12079000	0.11	0.10	0.090	15.5		36.8	0.1	(24)
HAT-196-0006238	17 58 59.3	+35 55 12						53623.7449	1.75834310				14.9				(9)
V924 Oph	18 33 28.3	+07 07 51							0.35955400					12.9			(5)
OT Lyr	19 08 10.0	+29 13 42						54222.4568	0.47109500					14.1			(5)
FP Sge	20 14 45.8	+19 36 49						52500.2947	0.64200717					14.0			(5)
NSVS 14256825	20 20 00.4	+04 37 56	0.46	0.21	sdo+M2		5.9	51288.9198	0.11037410	0.75	0.20	0.014	13.2	13.3	0.7	7.9	(25)
FI Del	20 29 16.0	+14 45 59						52500.3	0.41592810					14.6			(5)
MR Del	20 31 13.5	+05 13 08	0.69	0.63	K0V	0.01	3.7	52500.3087	0.52169040	0.33	0.17	0.073	11.0	8.9	1.4	2.7	(26)
RX J2130.6+4710	21 30 18.5	+47 10 07	0.55	0.55	M4V+WD		4.2	52785.6819	0.52103563	>2	0.00		13.0				(27)
HS 2231+2441	22 34 21.5	+24 56 57	0.30	0.30	sdB+dM		6.3		0.11058798				14.0	14.0			(28)
HAT-205-0007777	22 42 07.5	+39 02 44						53146.0021	1.11001010				14.6				(9)

Explanation of columns: α_{2000} , δ_{2000} - equatorial coordinates given for epoch and equinox 2000.0; $M_{1,2}$ - masses of the components; spectral classification; A_{OCC} - observed O'Connell effect amplitude expressed as difference in maxima levels; ΔT - amplitude of the LITE for 1 Jupiter mass planet orbiting the binary on 10 years orbit; HJD_I, Period - ephemeris for the primary (deeper) minimum; d_I , d_{II} - minima depth for the *I* passband (for the *V* passband typed in italics); D_I - duration of the primary eclipse; *V*, *R* - out-of-eclipse brightness of the binary; Δt - theoretically achievable minimum precision using a 60cm telescope (equation (4)) for the primary minima; $N_\sigma = \Delta T/\Delta t$ detection sensitivity of the binary.

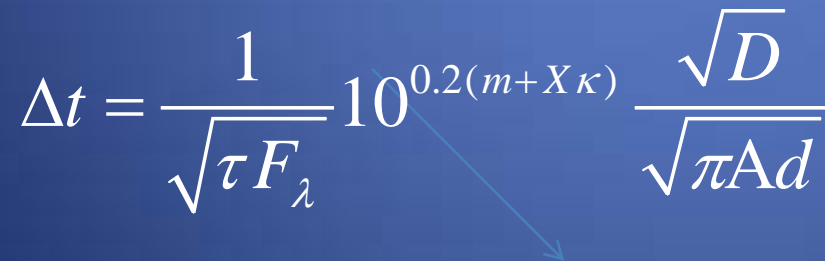
What are the chances to discover a circumbinary substellar body?

- i) precision and number of the minima which can be achieved
- ii) semi-amplitude of the LITE caused by the body
- iii) intrinsic variability of the binary causing noise in minima timings.

precision of a single minimum timing, Δt

$$\Delta t = \frac{D\sigma}{2d\sqrt{N}}$$


Diameter of telescope


$$\Delta t = \frac{1}{\sqrt{\tau F_{\lambda}}} 10^{0.2(m+X\kappa)} \frac{\sqrt{D}}{\sqrt{\pi A d}}$$


Henden & Kaitchuck, 1982

LITE amplitude

Max – Min or peak-to-peak changes

$$\Delta T \approx \frac{2M_3 G^{1/3}}{c} \left[\frac{P_3}{2\pi(M_1 + M_2)} \right]^{2/3}$$



Target	α_{2000}	δ_{2000}	M_1 [M_\odot]	M_2 [M_\odot]	Sp.type	A_{OCE} [mag]	ΔT [s]	HJD _I 2 400 000+	Period [days]	d_I [mag]	d_{II} [mag]	D_I [days]	V	R	Δt [s]	N_σ	Ref.
DV Psc	00 13 09.2	+05 35 43	0.49	0.51	K5V+M1V	0.04	4.5	52500.1150	0.30853740	0.32	0.15	0.062	10.6	10.0	1.1	4.1	(1)
PTFEB11.441	00 45 46.0	+41 50 30	0.51	0.35	M3.5+WD		5.0	55438.3165	0.35871000	0.20	0.00			16.3			(2)
NSVS 06507557	01 58 23.9	+25 21 20	0.66	0.28	K9+M3		4.7	54746.3801	0.51508836	0.70	0.23	0.062	13.4	12.6	1.8	2.6	(3)
BX Tri	02 20 50.8	+33 20 48	0.51	0.26	M1V+M4V	0.03	5.4	51352.0616	0.19263590	0.33	0.27	0.072	13.4	12.5	4.2	1.3	(4)
V449 Per	02 57 33.5	+35 14 01						52500.9069	0.94620690					12.5			(5)
GJ 3236	03 37 14.1	+69 10 50	0.38	0.28	M4V	0.02	5.9	54734.9959	0.77126000	0.21	0.19	0.039	14.0	13.5	6.3	0.9	(6)

in the case of a Jupiter-mass
planet orbiting the EB in 10 years

The suitability of an object (N_σ in Table 1) can be defined as the peak-to peak amplitude of LITE caused by such a body ΔT , divided by the theoretical precision of a single minimum timing, Δt



A. Papageorgiou, G. Katsoularis, & P.-E. Christopoulos
Biophysical Laboratory, Department of Physics, University of Patras, 26500, Patras, Greece

How to Contact Us

[illegible]

NAME: _____

[illegible]

PROFESSIONALISM IN ALABAMA

As an illustration we partitioned our available samples to *AXX* and *AXX_{neg}* (*AXX* vs *AXX_{neg}*) 170-fold. Using 10-fold cross-validation, we classified our random subsamples, *AXX_{neg}* class (50, 50, 50, 50, 50, 50, 50, 50, 50, 50). The performance of 10-fold cross-validation for the random subsamples is strong. For *AXX_{neg}* class, the sensitivity of 10-fold cross-validation is 0.99, specificity of 1.00, accuracy of 0.99, and the area under the ROC curve is 1.00. The results of 10-fold cross-validation for the subsamples, *AXX* class (50, 50, 50, 50, 50, 50, 50, 50, 50, 50) are not as good as the subsamples, *AXX_{neg}* class. The sensitivity, specificity, accuracy, and the area under the ROC curve are 0.99, 0.99, 0.99, and 1.00, respectively. This result suggests that the *AXX* class is more difficult to classify than the *AXX_{neg}* class. In this study, we use one sample to identify the tail of the distribution, whereas the sample size is small, and in this case, the sample size is 50. The results of 10-fold cross-validation for the subsamples, *AXX* class (50, 50, 50, 50, 50, 50, 50, 50, 50, 50) are not as good as the results of 10-fold cross-validation for the subsamples, *AXX_{neg}* class. Figure 2 presents the positions of *AXX_{neg}* and *AXX* in the distribution of the weights of random genes. *AXX_{neg}* and *AXX* are separated by the weights of random genes. *AXX_{neg}* is located in the left tail of the distribution, and *AXX* is located in the right tail of the distribution. This result suggests that the *AXX_{neg}* class is more difficult to classify than the *AXX* class.

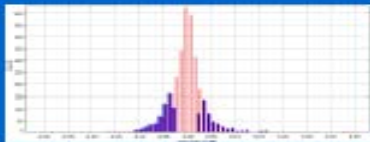


Figure 1. Histogram of the approximations for the sample. The bars with the light curves are performed to evaluate the outlying, whereas having OLS effect (Mars-Mars) > 0.025 may show one sample located in the tail of the distribution, whereas the approximation are true, to make not to represent an effect of fitting in every data (positive values of Mars-Mars as a result when Mars-Mars are equal and the fitting is performed in every data).

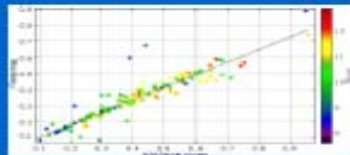


Figure 2. Coherence of fitting: indicated by the plot of the amplitude of variation given from ADAM definition and ADAM_{avg} against the amplitude of variation. Red was calculated from the fitting. Different colors presents the maximum magnitude of the outlying binary system.

¹<http://www.elsevier.com/locate/jbiomedeng>

1000-0000/01/0000-0000\$10.00/0

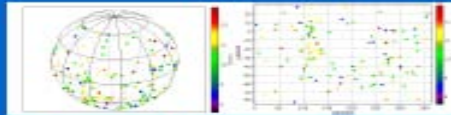
[illegible]

Figure 2. Representation of the distribution of the rolling moment adding to the ship. Different colors represent the maximum magnitude in Vt-head.

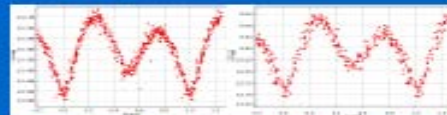


Figure 4. The representative examples, **ADACITION-08713** (a-f) and **ADACITION-07614** (g-h), of infusing honey bees (*Apis mellifera*) with strong, (C)Covad ethyl.

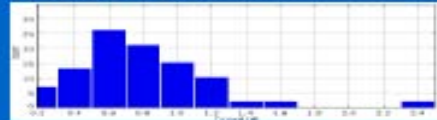


Figure 5. The period distribution of the existing money systems

[illegible]

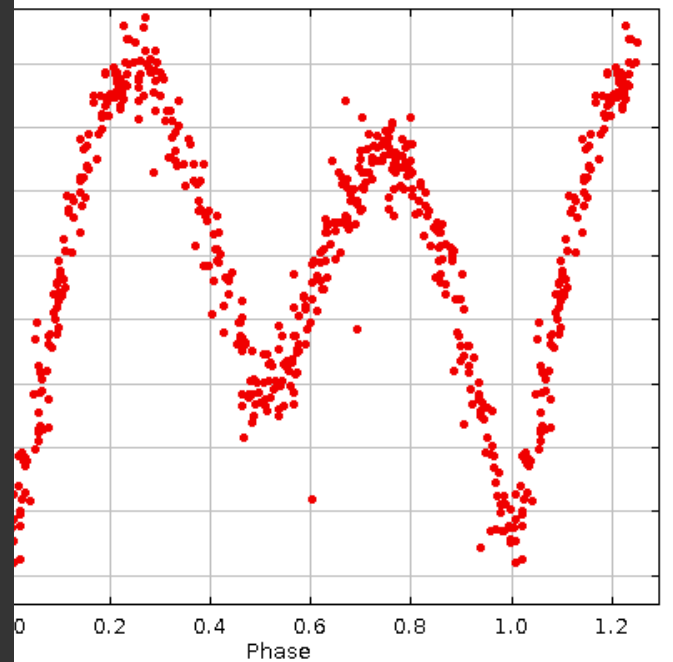
WILEY-INTERSCIENCE WILEY-SON

This automatic pipeline would be applied to other thickness maps, as in [KOPPELMAN, 2012](#) experiment 4b. The drawing system could be improved and more mathematical operations could be applied to order to ultimately find light curves or to search for other interesting morphological features (e.g. hole regions). It is also interesting to search for strong DCM-related effect in ranked datasets for monitoring purposes, in order to investigate

Acknowledgments: A. Pappagiovanni would like to thank G. Lucini Foundation for the support by postdoctoral fellowship.

100% **FREE** DELIVERY

Polymers 2019, 11, 1042



cover parts of the LC just before ingress and just after the egress from the minimum, examine period before

DATA reduction process

➤ CCD frames reduction

Reduction of Raw CCD frames, dark, flat-field frames, aperture photometry...

Resulting LC available on the DWARF page

➤ Reference time for the data

crucial to regularly synchronize the computer clock with the ntp servers to provide the system time within 1 second off the UTC...?... Barycentric Dynamical Time (TDB)

What about HJD (Heliocentric Julian Date) correction?

It is best to relate time to the Solar System Barycenter.

Hence we will use Barycentric Julian Dates in Barycentric Dynamical Time (BJD-TDB)

➤ Minima determination and uncertainties

Kwee & van Woerden (1956) method

Fitting function $F(x) = A + Bx + CT(x - D)$ (Pribulla et al. 2008)

Monte Carlo simulations

The timing analysis and its limitations

(O-C) curve (due only to the inner binary) can be described by a linear (constant period) or quadratic ephemeris (linear period variation) and if a third body is orbiting the inner binary adding the LITE effect, the times of the minima can be computed as follows (Irwin 1959)

$$\begin{aligned} \text{Min } I = & JD_0 + P \times E + Q \times E^2 + \\ & + \frac{a_{12} \sin i}{c} \left[\frac{1 - e^2}{1 + e \cos \nu} \sin(\nu + \omega) + e \sin \omega \right] \end{aligned}$$

α is the semi-major axis of the third (substellar) companion's orbit around the binary's mass center, then

$$a_{12} = \frac{a M_3}{M_1 + M_2 + M_3}.$$

Determination of orbital elements.....

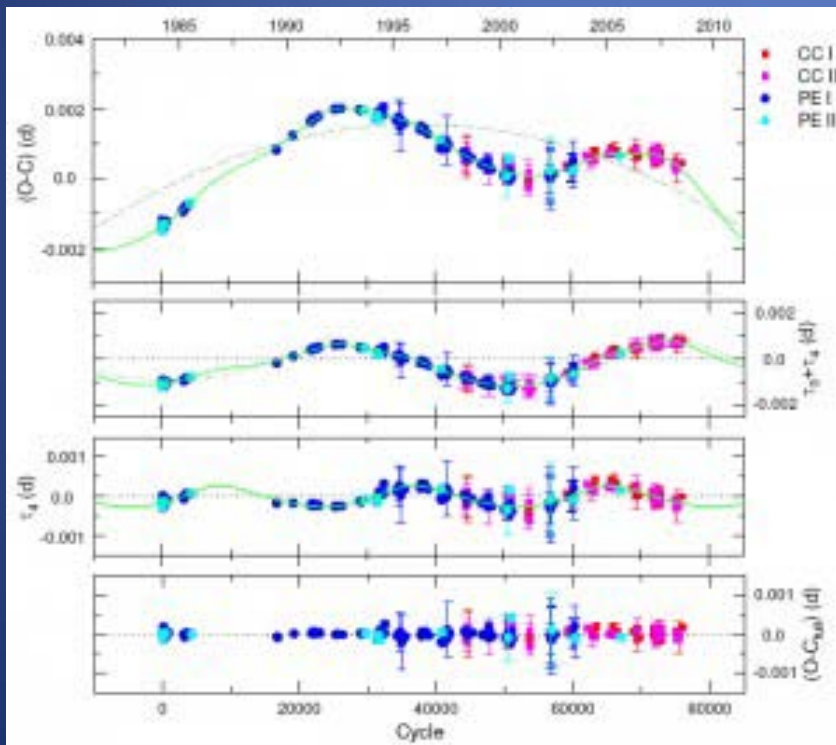
Derive the mass function of the third body

$$M_3^3 \sin^3 i \approx \frac{4\pi^2 (M_1 + M_2)^2}{GP_3^2} A^3 c^3$$

Eclipsing binary with confirmed planets

HW Vir (sdB and an M dwarf)

$P_{\text{orb}} = 2.8\text{h}$



- HW Vir, and the residuals of the eclipse timings measured since the early 1980s with respect to the linear terms of the Ibanoglu et al. (2004) ephemeris:
- (a) the parabolic curve corresponds to a linear period decrease, which might arise from magnetic stellar wind breaking;
- (b) residuals from the quadratic form;
- (c) residuals after including the effect of the 15.8 yr planet;
- (d) residuals with respect to the two-planet model. From Lee et al. (2009)

Stable configuration?

Horner & Hinse 2012

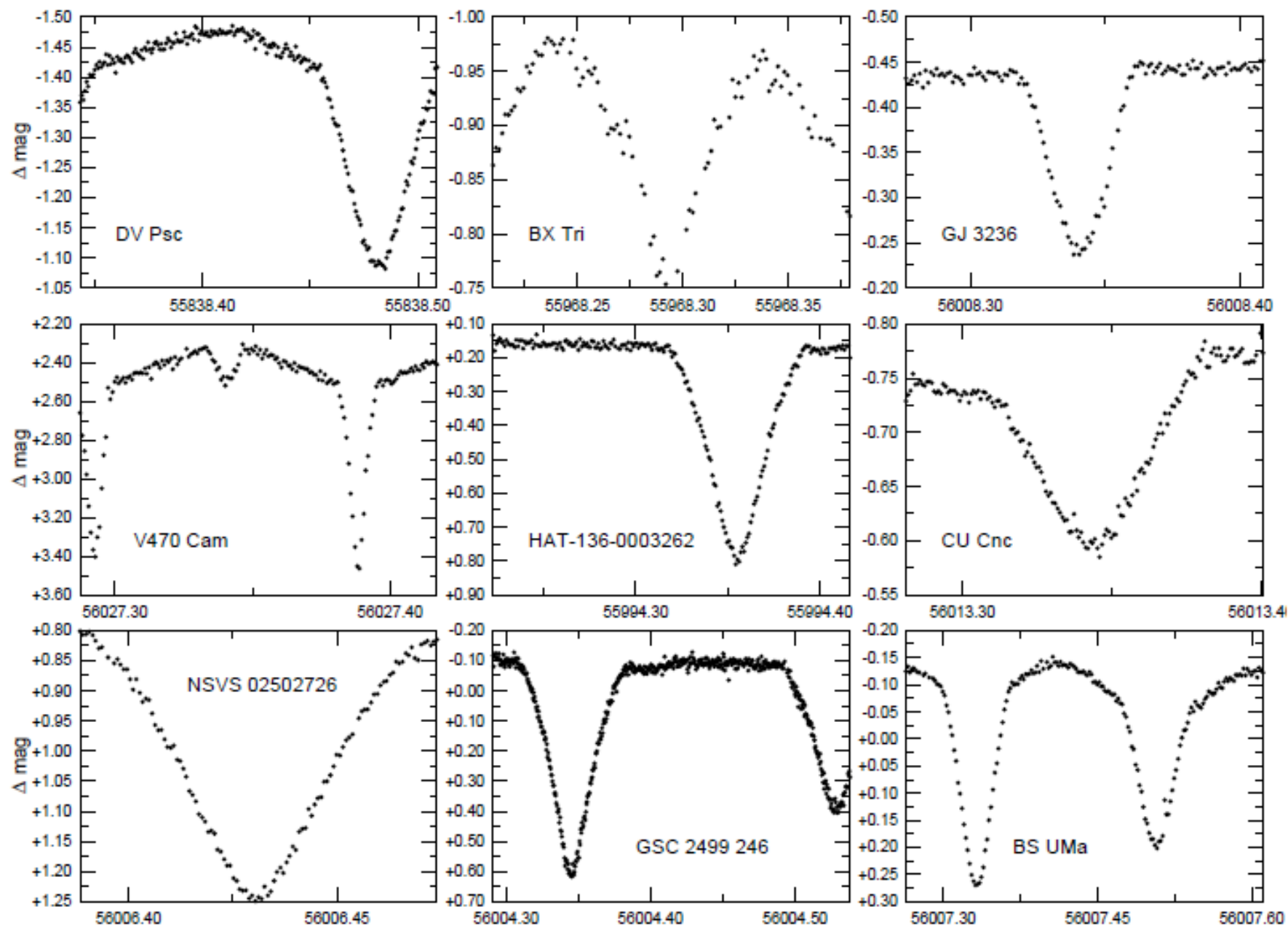
To further characterize the HW Vir system and constrain orbital parameters we recommend further observations within a monitoring program as described in Pribulla et al. (2012).

➤ Observing network and observations

- 35-120 cm telescopes with CCD cameras
- Targets DEC > -10°
- R or I filter for M or K EBs and V for sdB or WD components
- Short period cover both shoulders to see the LC asymmetry
- For most binaries with M and K dwarf component both minima
- WD component only primary

In addition...

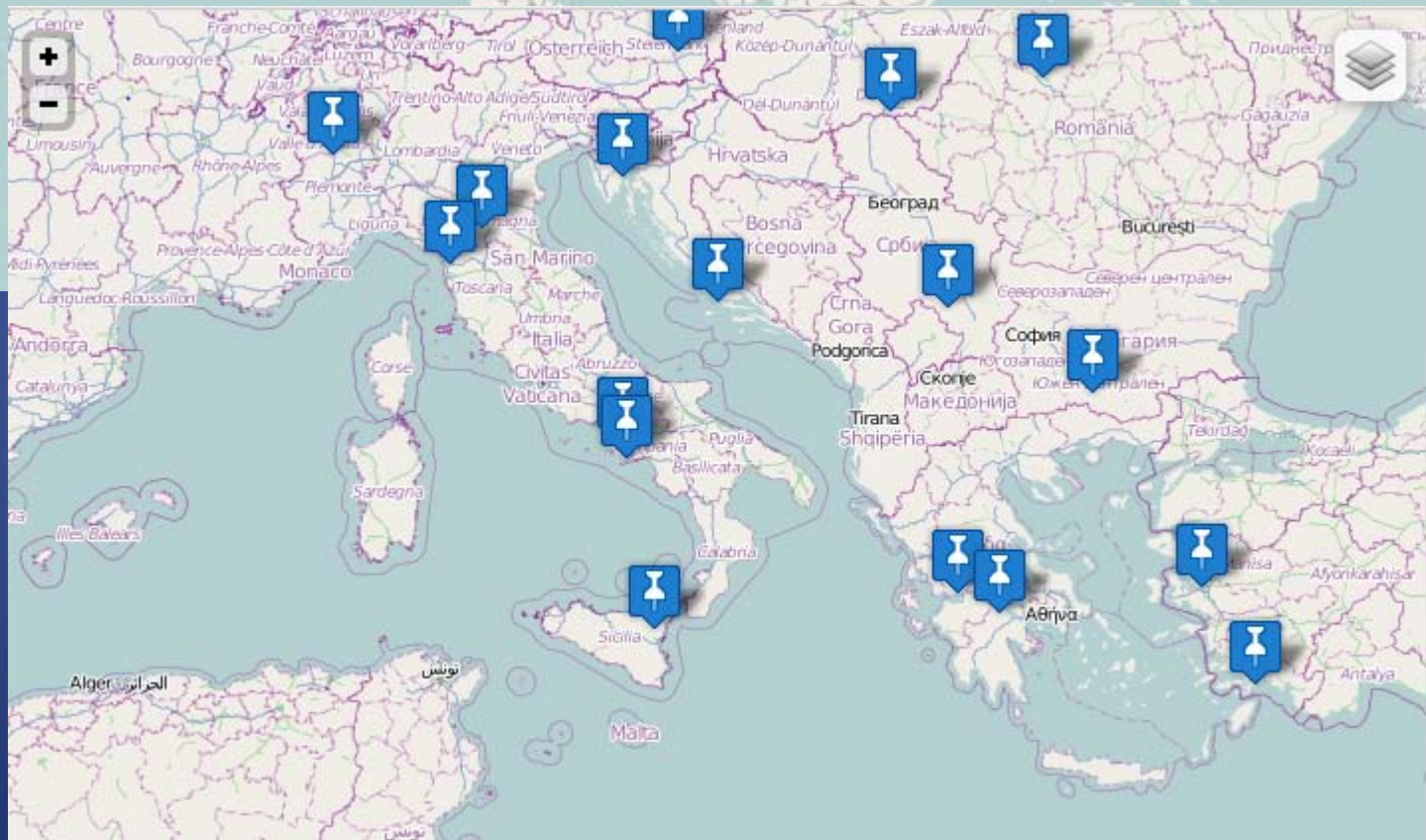
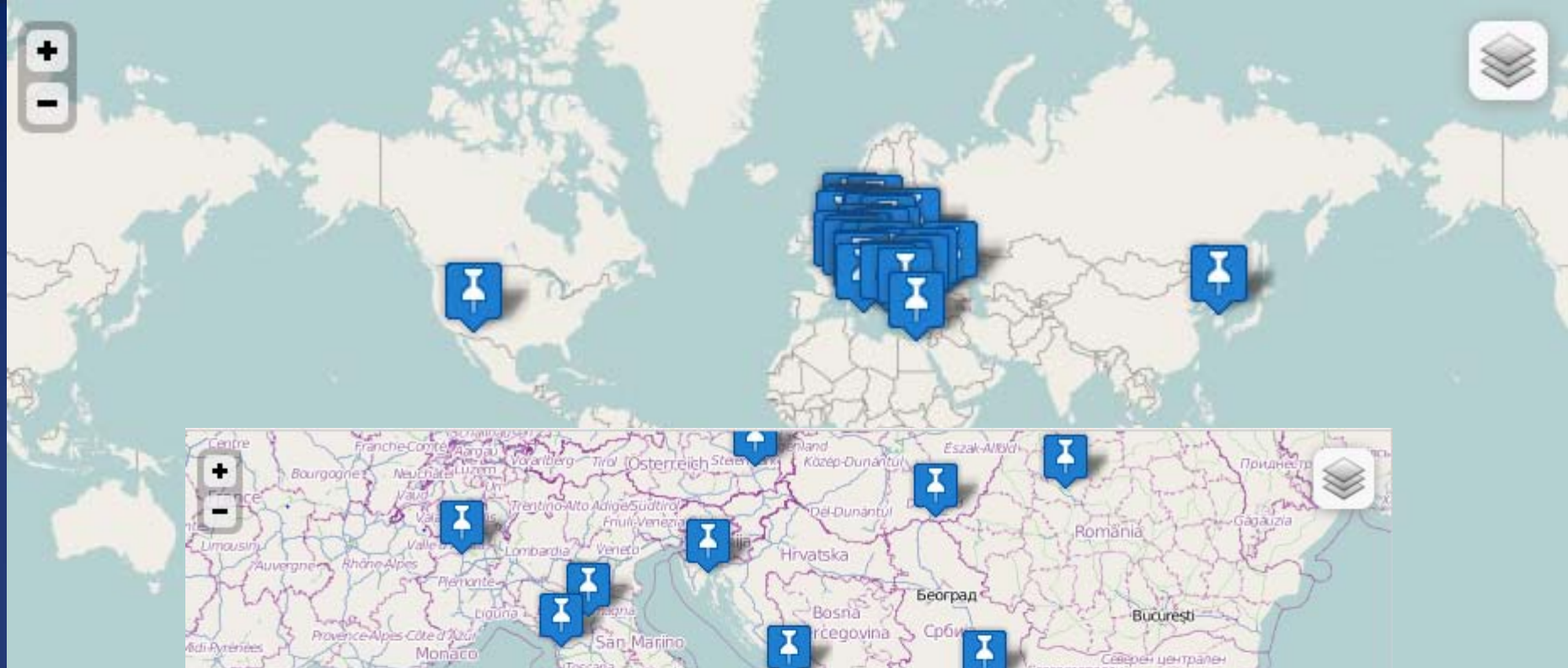
- “Extensive” multi-color UBVRI photometry Best comparison stars
Color brightness variations
- Medium to High resolution spectroscopy at the 2m telescope at Rozhen



Observing network and observations

Table 2 Telescope network (status as of April 22, 2012)

Observatory	Long. [deg.]	Lat. [deg.]	Telescope	Aperture [cm]	Camera	CCD size	FoV [arcmin]	Ref.
SOAO/Korea	128.4E	36.9N	Cassegrain	60	E2V CCD42-40	2048 × 2048	18 × 18	(1)
Terskol/Russia	42.5E	43.3N	Cassegrain	60	Pixel Vision	1024 × 1024	10 × 10	
			Schmidt-Cass.	35	SBIG STL-1001	1024 × 1024	24 × 24	
			Schmidt-Cass.	29	S3C	1024 × 1024	28 × 28	
OMU/Turkey	36.2E	41.4N	Schmidt-Cass.	35	STL-4020M	2048 × 2048	15 × 15	
Ankara/Turkey	32.8E	39.8N	Schmidt-Cass.	40	Apogee Alta U-47	1024 × 1024	11 × 11	(2)
Kottamia/Egypt	31.8E	29.9N	Cassegrain	188	EEV CCD 42-40	2048 × 2048	2.7 × 2.7	(3)
MAO NASU/Ukraine	30.5E	50.4N	Cassegrain	70	SBIG STL-1001	1024 × 1024	24 × 24	
Lesniki/Ukraine	30.5E	50.3N	Schmidt-Cass.	35	Rolera MG1	512 × 512	7 × 7	
ITAP/Turkey	28.3E	36.7N	Schmidt-Cass.	35	SBIG ST10 XME	2184 × 1472	14 × 10	(4)
Ege/Turkey	27.1E	38.4N	Schmidt-Cass.	40	Apogee CCD47-10	2048 × 2048	20 × 20	(5)
Rozhen/Bulgaria	24.7E	41.7N	Cassegrain	60	FLI ProLine 09000	3056 × 3056	17 × 17	(6)
			Schmidt	50/70	FLI ProLine 16803	4096 × 4096	73 × 73	
			Rit.-Chret.	200	Vers Array 1300B	1340 × 1300	5.7 × 5.7	
Feleacu/Romania	23.6E	46.7N	Schmidt-Cass.	40	SBIG STL-6303E	3072 × 2048	23 × 16	(7)
Kolonica	22.3E	48.9N	Cassegrain	100	FLI PL1001E	1024 × 1024	10 × 10	(8)
Slovakia			Schmidt-Cass.	35	MI G2-1600	1536 × 1024	12 × 8	
			Schmidt-Cass.	50	MI G4-16000	4096 × 4096	31 × 31	
Patras/Greece	21.7E	38.3N	Schmidt-Cass.	35	SBIG ST10 XME	2184 × 1472	20 × 14	
Astron. Station Vidojevica	21.5E	43.1N	Cassegrain	60	Apogee Alta U-42	2048 × 2048	16 × 16	(9)
Serbia			Cassegrain	60	Apogee Alta U-47	1024 × 1024	7.6 × 7.6	(10)
Roztoky/Slovakia	21.5E	49.4N	Cassegrain	40	MI G2-1600	1536 × 1024	12 × 8	
Stará Lesná	20.3E	49.2N	Newton	50	SBIG ST10 XME	2184 × 1472	20 × 14	(11)
Slovakia			Cassegrain	60	MI G4-9000	3056 × 3056	17 × 17	
Szeged/Hungary	20.2E	46.2N	Newton	40	SBIG ST7	765 × 510	17 × 11	
Torun/Poland	18.6E	53.1N	Cassegrain	60	SBIG STL-1001	1024 × 1024	12 × 12	
Bmo/Czech Rep.	16.6E	49.2N	Newton	62	SBIG ST8	1530 × 1020	17 × 11	
			Schmidt-Cass.	35	G2-4000	2056 × 2062		
Hvar/Croatia	16.4E	43.2N	Cassegrain	100	Apogee Alta U-47	2048 × 2048	8 × 8	(12)
Graz/Austria	15.5E	47.1N	Astro_Topar	30	SBIG STL11000M	4008 × 2672	16 × 11	
			Cassegrain	50	SBIG ST-2000XM	1600 × 1200	9 × 7	
Catania/Italy	15.0E	37.7N	Cassegrain	91	KAF1001E	1024 × 1024	12.5 × 12.5	(13)
			Rit.-Chret.	80	Apogee U9000	3040 × 3040	17 (diameter)	(14)
Prague/Czech Rep.	14.4E	50.1N	Schmidt-Cass.	40	SBIG ST10 XME	2184 × 1472	24 × 16	(15)
TLS/Germany	11.7E	51.0N	Schmidt	30	Apogee AP-16	4096 × 4096	132 × 132	(16)
Jena	11.5E	50.9N	Schmidt	60/90	E2V CCD42-10	2048 × 2048	53 × 53	(17)
Germany			Cassegrain	25	E2V CCD47-10	1056 × 1027	21 × 20	(18)
Kirchheim/Germany	11.0E	50.9N	Rit.-Chret.	60	SBIG STL-6303E	3072 × 2048	71 × 52	(19)
Herges-Hallenberg/Germany	10.6E	50.7N	Cassegrain	20	MI G2-1600	1536 × 1024	48 × 32	(20)
Trebur/Germany	8.4E	49.9N	Cassegrain	120	SBIG STL-6303E	3072 × 2048	10 × 7	(21)
LOAO/USA	110.7W	32.4N	Cassegrain	100	ARC 4K CCD	4096 × 4096	28 × 28	(22)



List of objects updated

Posted on [5. November 2012](#) | [Leave a comment](#)

New objects were added into list. The objects we

WD + M dwarf

■ SDSS

■ LP133

■ CSS 4

■ CSS 4

■ SW Se

low-mass bi

■ V641

■ KIC 5

■ KIC 6

[14. September 2012](#) | [Leave a comment](#)

Two objects were dropped from observational list:

OT Lyr shows just some ellipsoidal variations

Date	Object	Observatory	Instrument	Filter(s)	Light curve
2012-10-01	GJ 3236	Patras	Schmidt-Cassegrain	Ic	View Download
2012-09-30	GJ 3236	Patras	Schmidt-Cassegrain	Ic	View Download
2012-09-30	BX Tri	Patras	Schmidt-Cassegrain	Ic	View Download
2012-09-29	GJ 3236	Patras	Schmidt-Cassegrain	Ic	View Download
2012-09-29	BX Tri	Patras	Schmidt-Cassegrain	Ic	View Download
2012-09-29	AP Tau	Patras	Schmidt-Cassegrain	Ic	View Download
2012-09-28	GJ 3236	Patras	Schmidt-Cassegrain	Ic	View Download
2012-09-28	BX Tri	Patras	Schmidt-Cassegrain	Ic	View Download
2012-09-28	CM Dra	Patras	Schmidt-Cassegrain	Ic	View Download
2012-09-27	BX Tri	Patras	Schmidt-Cassegrain	Ic	View Download
2012-09-27	AP Tau	Patras	Schmidt-Cassegrain	Ic	View Download
2012-09-27	YY Gem	Patras	Schmidt-Cassegrain	Ic	View Download
2012-09-26	GI 3236	Patras	Schmidt-Cassegrain	Ic	View Download
2013-08-10	HS 2231+2441	MAO NASU	Celestron	Clear	View Download
2013-08-10	FP Sge	Lesniki	Schmidt-Cassegrain	Clear	View Download
2013-08-10	G179-55	Lesniki	Schmidt-Cassegrain	R	View Download
2013-08-09	GU Boo	Lesniki	Schmidt-Cassegrain	R	View Download

Conclusion

Additional useful science

- the study of spot cycles in the RS CVn-like late-type binaries, detection of flares (see Pribulla et al., 2001)
- A more accurate characterization of recently discovered detached eclipsing binaries
 - detection of new low-mass EBs which is crucial to better define the empirical lower main sequence
- determination of absolute parameters of the components (in the case that spectroscopic orbits are available)
 - detection of EBs with pulsating component(s)
- detection and characterization of multiple systems with two systems of eclipses
 - detection of new variable stars in the CCD fields covered
- Photometric detection of transits of substellar components across the disks of the components of the eclipsing pair (see Doyle et al., 2011)
 - detection of invisible massive components causing precession of the EB orbit and changes of the minima depth (see Mayer et al., 2004).

Last but not least...

Aristarchos observations July-August 2013

